Influence of Crack Depth on Dynamic Characteristics of Spur Gear System

Yuan Chen [1,2], Rupeng Zhu [1,*], Guanghu Jin [1], Yeping Xiong[2]

[1] National Key Laboratory of Science and Technology on Helicopter Transmission, Nanjing, 210016, China

rpzhu@nuaa.edu.cn

[2] Engineering and the Environment, University of Southampton, Boldrewood Innovation Campus SO16 7QF, Southampton United Kingdom

Abstract

Root crack is relatively common failure scenarios in spur gear system, and its dynamic characteristics and crack identification theory are addressed by many scholars. However, cracked spur gear identification model, especially related to its signal propagation characteristics, requires in-depth research due to the limited published works. Therefore, a bending-torsional coupling nonlinear vibration model of six degrees of freedom (DOF) is established through lumped mass method. Besides, the influence of tooth root crack on the measuring point signal is considered in the model. The time domain response of the system is solved by Runge-Kutta numerical integration method, and the frequency domain characteristics are obtained. The change of different tooth-root crack depth on the response amplitude of measuring points is studied; According to the system identification theory of 6th ARX model, the transfer function of vibration signal propagation paths between the measuring points is obtained, and the influence of cracks on transfer function is analyzed. The research provides a theoretical basis for the system testing and measuring point's parameter identification.

1 Introduction

Gear transmission is quite widely applied in automotive, aerospace and ship, it is featured with strong bearing capacity and compact structure. However, the gear fault is frequent because transmission parts are under the influence of transient impact and alternating load[1,2]. Crack is one of the early fault forms of gears. To timely and accurately find and locate the fault, and eliminate hidden dangers is of great significance for improving the efficiency of gear system[3-5].

In the area of gear fault analysis, some early studies focused on the meshing stiffness of healthy gears[6-10], these studies were the basis in the calculation of fault gear's meshing stiffness[11]. O. Mohammed *et al.*[12-17] established gear root assumption and studied three different series of crack propagation. X. Zhou *et al.*[18] investigated the response of a spur gear system, and time-varying meshing stiffness with pinion cracking were taken into consideration. I. Yesilyurt *et al.*[19-20] derived a non-destructive technique for spur gear

* Corresponding author.

damage detection and severity assessment in the vibration analysis. N. Raghuwanshi *et al.*[21] studied a three-dimensional model of a spur gear pair through finite element method (FEM) when gear teeth are under back-side contact.

Some other researchers focused on gear signal identification, which is widely used in detection of failures. N. Baydar *et al.*[22] investigated that acoustic signals have strong effect on the early detection. J. Wu *et al.*[23] described the fault gear identification system with discrete wavelet transform technique and fuzzy–logic inference, the experimental results validated the high recognition rate. Y. Lei *et al.*[24-25] proposed a weighted K nearest neighbor (WKNN) classification algorithm for identifing the crack levels. M. Yang *et al.*[26] presented ARX model to localize the pending failure for gearbox under varying load conditions.

Based on the above-mentioned studies, to locate crack fault through the vibration signals of the measuring points and explore the transmission characteristics of crack fault with different depth is meaningful for gear system. ARX model could be applied to analyze spur gears' propagation characteristics under different scenarios of crack, however, it has not been investigated in the previous research.

In the paper, the dynamic model of bending- torsional coupling gear system is established. Besides, the impact of the crack depth on time-varying meshing stiffness is explored; the numerical calculation is conducted on theoretical vibration response of each measuring point, and system propagation characteristics are analyzed through ARX identification model to assist fault identification.

2 Mathematical Modelling

2.1 Dynamic model of the system

A dynamic model of bending-torsional spur gear system is shown in Fig.1, the measuring points are arranged at the bearing of the input and output respectively, and the system has 6 degrees of freedom[27], which could be defined as $X=\{Y_p, Y_g, \theta_p, \theta_g, \theta_m, \theta_b\}^T$. Here, θ_p and θ_g are rotational DOF of driver gear and driven gear; θ_p and θ_g are rotational DOF of input engine and output load.

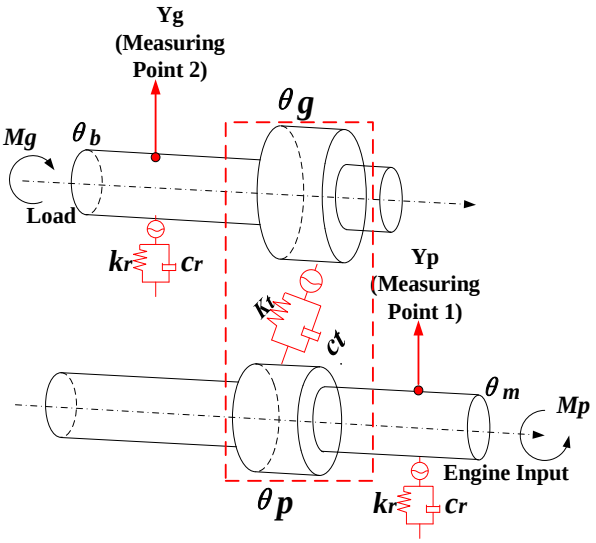

Fig.1 Dynamic model

The relative displacement along the gear meshing line is defined as follows:

$$X = R_p\theta_p - R_g\theta_g - Y_p + Y_g \tag{1}$$

Taking dynamic meshing force, input torque M_p and output load M_d and some other internal and external excitations into account, the system differential equation can be deduced:

$$\begin{cases} m_p\ddot{Y}_p = -c_r\dot{Y}_p - k_rY_p + k_tX + c_t\dot{X} \\ m_g\ddot{Y}_g = -c_r\dot{Y}_g - k_rY_g + k_tX + c_t\dot{X} \\ I_p\ddot{\theta}_p = c_c(\dot{\theta}_m - \dot{\theta}_p) + k_c(\theta_m - \theta_p) - R_p(k_tX + c_t\dot{X}) \\ I_g\ddot{\theta}_g = c_c(\dot{\theta}_b - \dot{\theta}_g) + k_c(\theta_b - \theta_g) + R_g(k_tX + c_t\dot{X}) \\ I_m\ddot{\theta}_m = M_p - k_c(\theta_m - \theta_p) - c_c(\dot{\theta}_m - \dot{\theta}_p) \\ I_b\ddot{\theta}_b = M_g + k_c(\theta_g - \theta_b) + c_c(\dot{\theta}_g - \dot{\theta}_b) \end{cases} \tag{2}$$

here, c_r is supporting damping of the bearing; k_r is supporting stiffness of the bearing; k_t is meshing stiffness; c_t is meshing damping; k_c is shaft torsional stiffness; c_c is torsional damping of the shaft.

2.2 Time-varying meshing stiffness considering crack depth

The crack normally happens at the root of the gear[9], which is shown in Fig.2. Crack parameter q_0 is the depth of the crack. After crack fault appears, gear meshing deformation would change, and then the stiffness would change. For the calculation of the deformation, the gear teeth are regarded as a cantilever beam. Deformation generally included shear deformation, bending deformation, axial deformation, etc.

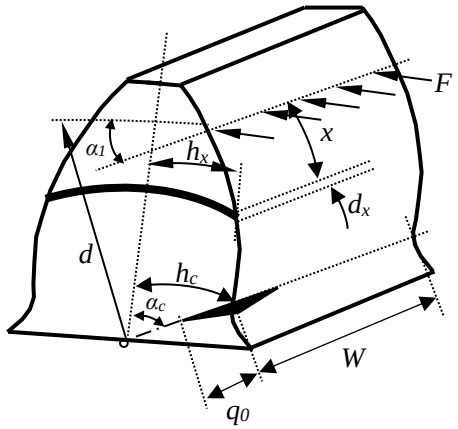

Fig.2 Model of gear tooth crack

Bending, shear, and axial compressive meshing stiffnesses of cracked gear are defined as [9]:

$$\begin{cases} \dfrac{1}{K_b} = \displaystyle\int_0^d \frac{[x\cos(\alpha_1) - h\sin(\alpha_1)]^2}{EI_x}\,dx \\ \dfrac{1}{K_s} = \displaystyle\int_0^d \frac{1.2\cos^2(\alpha_1)}{GA_x}\,dx \\ \dfrac{1}{K_a} = \displaystyle\int_0^d \frac{\sin^2(\alpha_1)}{GA_x}\,dx \end{cases} \tag{3}$$

where K_b is bending stiffness; K_s is shear stiffness; K_a is axial stiffness; E is Young's modulus; G is shear modulus; Other length parameters h_c, h_x, α_c and α_1 are all shown in Fig.2.

I_x and A_x are defined as:

$$I_x = \begin{cases} (1/12)(h_x + h_x)^3 dW, & h_x \le h_q \\ (1/12)(h_x + h_q)^3 dW, & h_x > h_q \end{cases}$$
$$A_x = \begin{cases} (h_x + h_x) dW, & h_x \le h_q \\ (h_x + h_q) dW, & h_x > h_q \end{cases} \quad (4)$$

here, h_q=h_c-$q_0$sin(α_c).

According to Equation (3-4), the total meshing stiffness of the corresponding crack is:

$$K(m) = 1/\left(\frac{1}{K_b} + \frac{1}{K_s} + \frac{1}{K_a}\right) \quad (5)$$

Fig.3 shows the meshing stiffness under different crack depth through simulation calculation. Based on the figure, with the increase of crack depth, meshing stiffness of the single-tooth meshing area and the double-tooth meshing area are both reduced because the change of crack depth increased gear deformation, thus decreasing stiffness value. In addition, as seen from Fig.3 (a-b), the calculated meshing stiffness of different crack sizes show gradually decreased or increased depending on the cracked gear is the driver or driven gear.

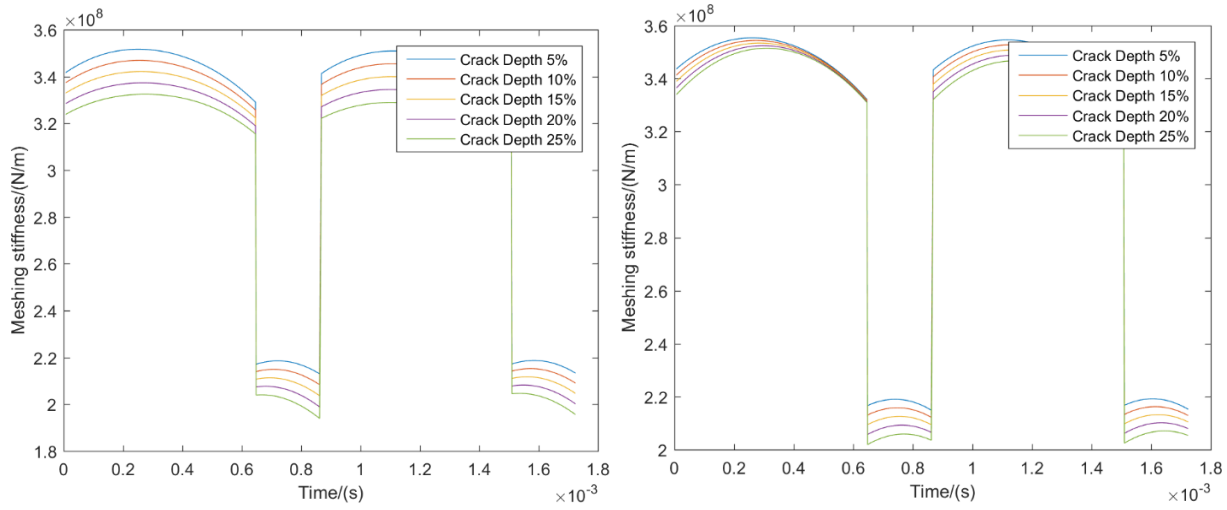

(a)Driver gear crack (b)Driven gear crack

Fig.3 Meshing stiffness influenced by different crack depth

3 Calculation

3.1 Influence of Crack Depth on Response Spectrum

The parameters of a geared system are listed in Table 1. In addition, the engine input power is 3kW and maximum input speed is 2400r/min. Gear parameters and working conditions are based on the test gearbox of helicopter transmission technology laboratory in Nanjing University of Aeronautics and Astronautics (NUAA).

Table.1 System Parameters

Parameter	Driver Gear	Driven Gear

Modulus	1.5	
Pressure angle (°)	20	
Tooth number	29	100
Face width(m)	0.04	0.04
Young's modulus (N/m^2)	2.1×10^{11}	
Poisson's ratio	0.269	
Shaft torsional stiffness (N·m/rad)	4.4×10^{4}	
Bearing Supporting stiffness (N/m)	6.56×10^{7}	4.78×10^{7}
Shaft torsional damping (N•s/m)	5×10^{5}	
Bearing Supporting damping (N•s/m)	1.8×10^{5}	

In this paper, the Runge-Kutta method is applied to solve the above-mentioned differential equation (Equation 2), and the steady-state response in the time domain of measuring point 1 and measuring point 2 is obtained. The signals of first 300 transient responses are omitted, and the frequency domain map is drawn by fast Fourier transform (FFT). So responses of measuring point 1 and point 2 in the crack-free state are shown in Fig.4.

As seen in Fig.4 (a-b), signals at the measuring point 1 and point 2 present the periodic change; the response of the measuring point 2 under the condition of the time domain is greater than that of the measuring point 1. According to Fig.4 (c-d), the vibration signals are dominated by its meshing frequency (1160Hz), and there is also a peak in the double frequency (2320Hz), triple frequency (3480 Hz) and quadruple frequency (4640Hz). For low frequency, which is smaller than 1000Hz, the response of measuring point 2 is much greater than measuring point 1, and the value changes remarkably.

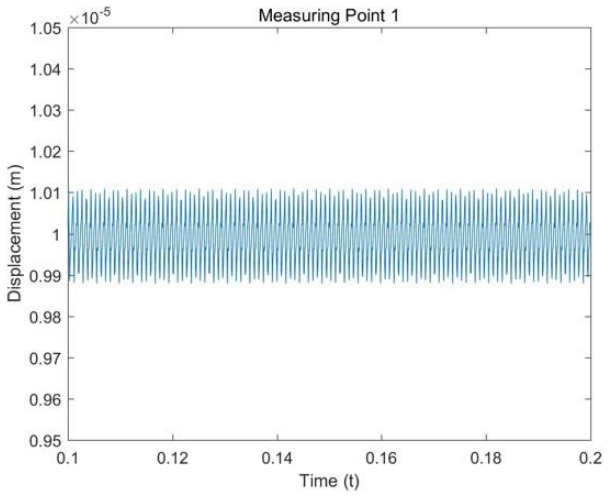

(a) Time domain of MP1

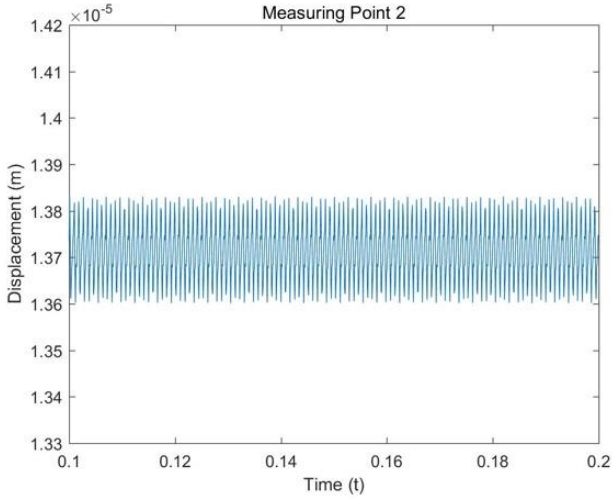

(b)Time domain of MP2

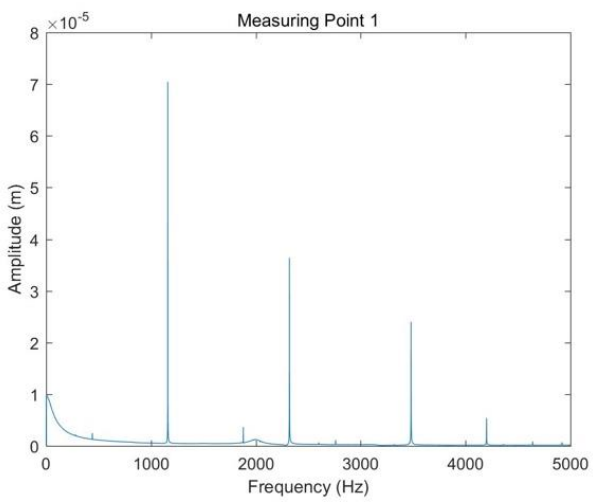

(c) Frequency domain of MP1

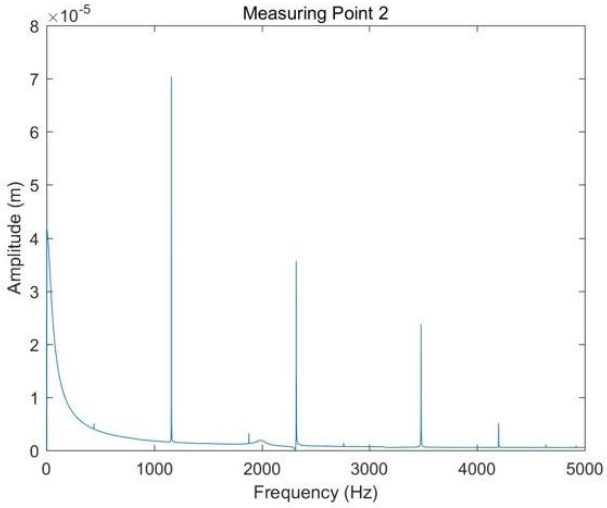

(d) Frequency domain of MP2

Fig.4 Responses of measuring points in crack-free state

The same numerical method are used for solving the signal response spectrum of the measuring points (MP) with different driver gear's crack depth, as shown in Fig.5. As seen from Fig.5 (a-c), there were a massive sideband components surrounding each doubling meshing frequency. In addition, Fig.5 (b) and Fig.5 (d) show that there was a local peak at 2000Hz because of the influence of the crack; the signal was very weak when there was no crack; as the crack length increases, the peak rose sharply; when crack depth was more than 25%, the crack signals were very obvious on the FFT spectrum, and they were close to the peak of three times frequency. Therefore, the measuring point 1 and 2 were sensitive to cracks, and they could be regarded as one of the judgment basis of early crack deterioration. However, when the frequency was below 1000Hz, the base signal rate of the measuring point 1 was small, and the spectrum changes caused by crack signals became more clear. Thus. The measuring point 1 was the best measuring point.

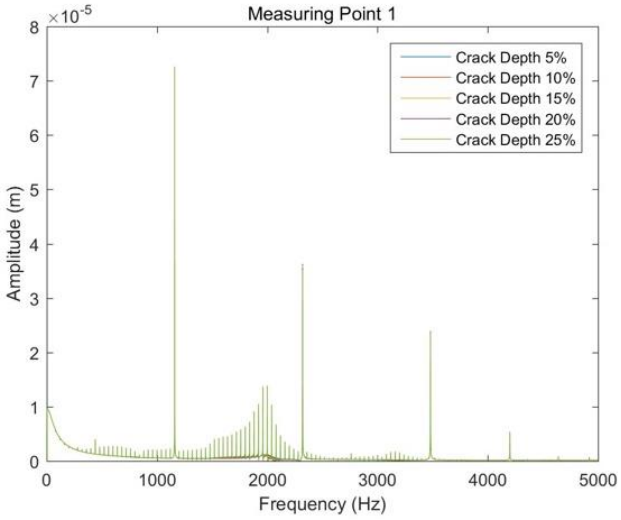

(a) Complete frequency domain of MP1

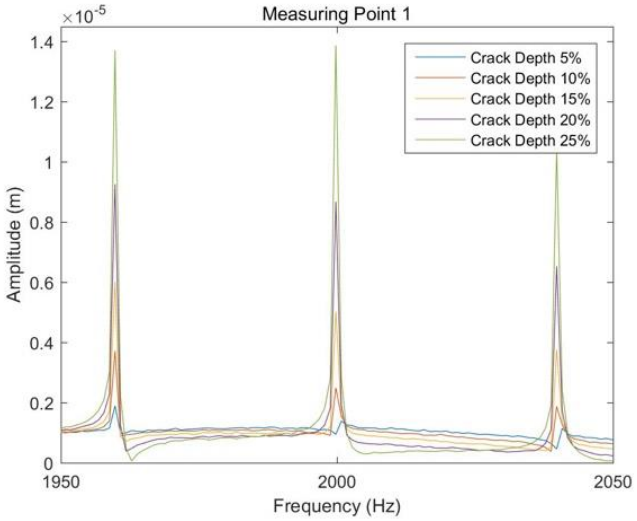

(b) Partial frequency domain of MP1

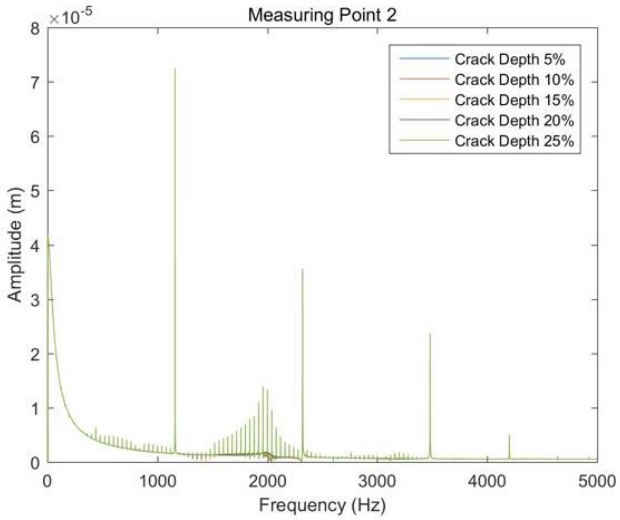

(c) Complete frequency domain of MP2

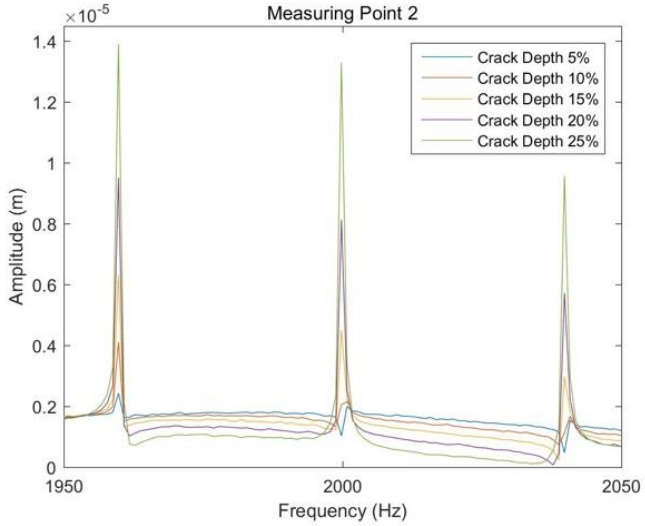

(d) Partial frequency domain of MP2

Fig.5 Spectrum of measuringd point in different crack state

3.2 Influence of Crack Depth on Transfer Function

1) ARX parameter identification model

In the field of engineering technology, the general model that is used to describe the dynamic characteristics of the discrete system is n order difference equation. For a so-called input/output 'black box' system, the most general expression of its difference equation can be defined as follows:

$$A(z)y(k) = B(z)u(t-nk) + e(k) \tag{6}$$

where, $u(k)$ and $y(k)$ are the signals of the input and output, $e(k)$ is the noise signal. $A(z)=1+a_1z^{-1}+a_2z^{-2}+a_nz^{-n}$, $B(z) =b_1+ b_2z^{-1}+b_3z^{-2}+b_nz^{-n}$, they are z-transform form; n denotes order for recognition. In order to improve the recognition accuracy, the order could be accordingly improved. 6-order ARX identification model was adopted in the paper. a_n and b_n identification results were solved as shown in Table 2. According to the table, with the increase of crack depth, precision reduces slightly, but the overall precision is greater than 99.40%.

Table.2 Input and output identification results

	A(z)	B(z)	Identification Precision
Crack Depth5%	$1 + 0.04581z^{-1} - 0.1591z^{-2} - 0.06681z^{-3} + 0.1104z^{-4} - 0.9063z^{-5} + 0.089z^{-6}$	$0.9341 + 0.173z^{-1} - 0.1892z^{-2} - 0.06399z^{-3} + 0.1525z^{-4} - 0.8901z^{-5} + 0.03885z^{-6}$	99.44%
Crack Depth10%	$1 + 0.06386z^{-1} - 0.1557z^{-2} - 0.06808z^{-3} + 0.1058z^{-4} - 0.9102z^{-5} + 0.07951z^{-6}$	$0.9332 + 0.1907z^{-1} - 0.1845z^{-2} - 0.06458z^{-3} + 0.1476z^{-4} - 0.8933z^{-5} + 0.02883z^{-6}$	99.43%
Crack Depth15%	$1 + 0.09253z^{-1} - 0.1527z^{-2} - 0.06962z^{-3} + 0.1028z^{-4} - 0.9163z^{-5} + 0.06187z^{-6}$	$0.9317+ 0.2192z^{-1} - 0.1795\ z^{-2} - 0.0653z^{-3} + 0.144z^{-4} - 0.8975z^{-5} + 0.01025z^{-6}$	99.43%
Crack Depth20%	$1 + 0.1378z^{-1} - 0.1538z^{-2} - 0.07221\ z^{-3} + 0.1031z^{-4} - 0.923z^{-5} + 0.03203\ z^{-6}$	$0.929 + 0.2648z^{-1} - 0.1775z^{-2} - 0.06713z^{-3} + 0.1427z^{-4} - 0.9009z^{-5} - 0.02098z^{-6}$	99.42%

Crack Depth25%	$1 + 0.1984z^{-1} - 0.1616z^{-2} - 0.07407z^{-3} + 0.1103z^{-4} - 0.931z^{-5} - 0.01135z^{-6}$	$0.9251 + 0.3265z^{-1} - 0.1813z^{-2} - 0.06859z^{-3} + 0.1475z^{-4} - 0.9033z^{-5} - 0.06638z^{-6}$	99.40%

2) Bode Graph of Transfer function

The transfer function of the system after identification is solved as well. Besides, the bode diagram is drawn, the relationship between the signal increment and frequency of input and output are obtained. Based on Fig.6 (a), the change of crack depth on the input and output signal transfer function is not obvious, that is because two measuring points and crack signals are at the same retarding stage and transmission distance is short. At the same time, as seen from the partial diagram of Fig.6 (b), with the increase of crack depth, partial transfer function amplitude shows gradually decrease. As the deep cracks changes the input signal and output signal amplitude considerably, and the signal increment effect is not obvious, the transmission characteristics of the system would be reduced with the increase of crack depth.

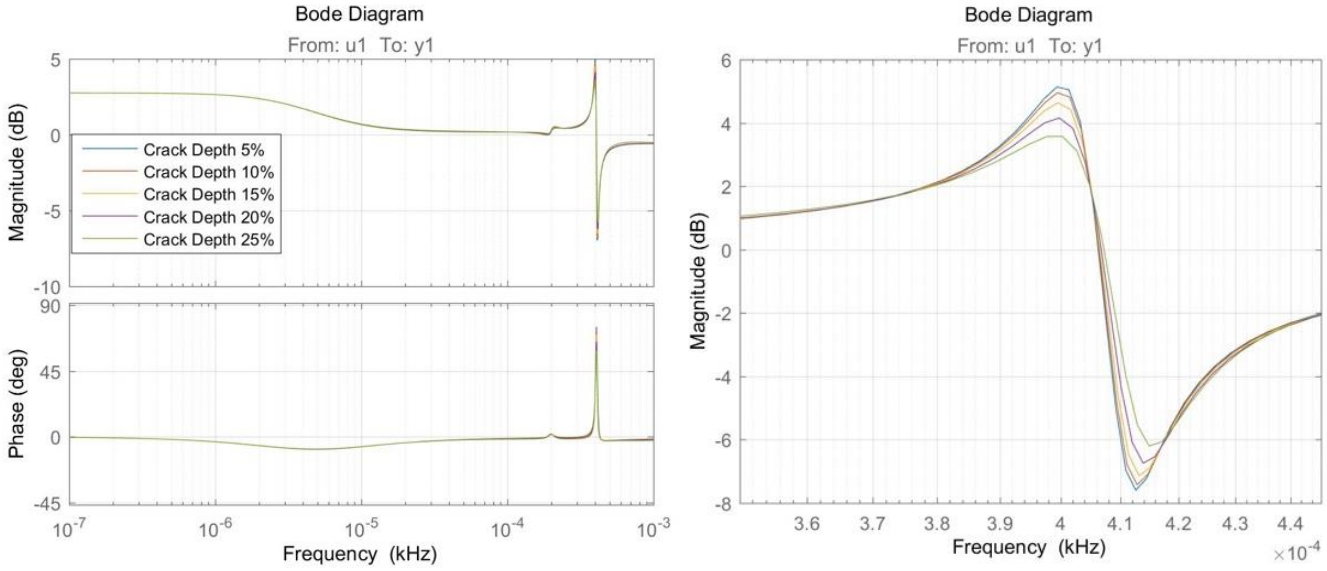

(a) Complete frequency domain (b) Partial frequency domain

Fig.6 Influence of crack depth on system transfer characteristics

4. Conclusion

With calculated high identification precision, this paper provides a new and effective method in sloving gear crack identification problems, which makes it a great contribution to spur gear dynamic analysis system. Some crucial conclusions and results are shown as follows:

(1) With the increase of crack length, meshing stiffness of single-tooth mashing area and double-tooth meshing area reduced.

(2) When the frequency was lower than 1000Hz, the response amplitude of the measuring point 1 was less than that of the measuring point 2, and the signal peak change relatively slightly. When crack signals occurred, it was simple to distinguish them. When the frequency was above 1000Hz, the two measuring points had similar crack signal recognition ability. Therefore, the measuring point 1 was the best measuring point.

(3) When cracks appeared, there were a massive sideband components surrounding each doubling meshing frequency. A local peak emerged at 2000Hz; with the progressive increase of cracks, the peak increased

rapidly.

(4) With the increase of crack depth, precision reduces slightly, but the overall precision calculated by 6-order ARX identification model is greater than 99.40%.

(5) The increasement effect of the signal input and output is not obvious; the system transfer characteristics becomes poor.

5 Acknowledgments

This research is supported by the National Natural Science Foundation of PRC (No. 51775265); Postgraduate Research and Practice Innovation Program of Jiangsu Province (Grant KYCX17_0242); China Scholarship Council.

Reference

[1] Li X., You B., Zhang H. and Zhao Y., Dynamic Analysis of Gear-rotor System Coupled with Radial Clearance and Dynamic Backlash, *Journal of Vibration Engineering & Technologies*, Vol.4, pp. 271-281, 2016.

[2] Li F., Zhu R., Bao H., Jin G. and Guan Q., The Analysis on Influence of Nonlinear Dynamics Characteristics for Gears System Caused by Contact Ratio, *Journal of Vibration Engineering & Technologies*, vol.3, pp. 551-563, 2015.

[3] Wu, S., Zuo, M., and Parey, A., Simulation of spur gear dynamics and estimation of fault growth, *Journal of Sound and Vibration*, Vol.317, pp. 608-624, 2008.

[4] Li, C., and Lee, H., Gear fatigue crack prognosis using embedded model, gear dynamic model and fracture mechanics, *Mechanical systems and signal processing*, Vol.19, pp. 836-846, 2005.

[5] Kumar, H., Sugumaran, V. and Amarnath M., Fault Diagnosis of Bearings through Sound Signal Using Statistical Features and Bayes Classifier, *Journal of Vibration Engineering & Technologies*, Vol. 4, pp. 87-96, 2016.

[6] Weber, C., The deformation of loaded gears and the effect on their load carrying capacity, Sponsored Research (Germany), *British Dept. of Scientific and Industrial Research*, 1949.

[7] Attia, A., Deflection of spur gear teeth cut in thin rims, *Journal of Engineering for Industry*, Vol. 86, 1963.

[8] Kasuba, R. and Evans J., An extended model for determining dynamic loads in spur gearing, *Journal of mechanical design*, Vol.103, pp. 398-409, 1981.

[9] Lin, J., Hertzian damping, tooth friction and bending elasticity in gear impact dynamics, 1987.

[10] Özgüven, H. and Houser, D., Mathematical models used in gear dynamics—a review, *Journal of sound and vibration*, Vol.121, pp. 383-411, 1988.

[11] Chen, Z. and Shao, Y., Dynamic simulation of spur gear with tooth root crack propagating along tooth width and crack depth, *Engineering Failure Analysis*, Vol.18, pp. 2149-2164, 2011.

[12] Mohammed, O., Rantatalo, M., Aidanpää, J. and Kumar, U., Vibration signal analysis for gear fault diagnosis with various crack progression scenarios, *Mechanical systems and signal processing*, Vol.41, pp. 176-195, 2013.

[13] Mohammed, O., Rantatalo, M. and Aidanpää, J., Dynamic modelling of a one-stage spur gear system and vibration-based tooth crack detection analysis, *Mechanical Systems and Signal Processing*, Vol.54, pp. 293-305, 2015.

[14] Mohammed, O., Rantatalo, M. and Aidanpää, J., Improving mesh stiffness calculation of cracked gears for the purpose of vibration-based fault analysis, *Engineering Failure Analysis*, Vol.34, pp. 235-251, 2013.

[16] Mohammed, O. and Rantatalo, M., Gear tooth crack detection using dynamic response analysis, *Insight*, Vol.55, pp. 417-421, 2013.

[17] Mohammed, O., Rantatalo, M. and Kumar, U., Analytical crack propagation scenario for gear teeth and time-varying gear mesh stiffness, *World Academy of Science, Engineering and Technology*, 2012.

[18] Zhou, X., Shao, Y., Lei, Y. and Zuo, M., Time-varying meshing stiffness calculation and vibration analysis for a 16 DOF dynamic model with linear crack growth in a pinion, *Journal of Vibration and Acoustics*, Vol.134, pp. 011011, 2012.

[19] Yesilyurt, I., Gu, F. and Ball, A., Gear tooth stiffness reduction measurement using modal analysis and its use in wear fault severity assessment of spur gears, *NDT & E International*, Vol.36, pp. 357-372, 2003.

[20] Ozturk, H., Yesilyurt, I. and Sabuncu, M., Investigation of effectiveness of some vibration-based techniques in early detection of real-time fatigue failure in gears, *Shock and Vibration*, Vol.17, pp. 741-757, 2010.

[21] Raghuwanshi, N. and Parey, A., Effect of Back-side Contact on Mesh Stiffness of Spur Gear Pair by Finite Element Method, *Procedia Engineering*, Vol.173, pp. 1538-1543, 2017.

[22] Baydar, N. and Ball, A., Detection of gear failures via vibration and acoustic signals using wavelet transform, *Mechanical Systems and Signal Processing*, Vol.17, pp. 787-804, 2003.

[23] Wu, J. and Hsu, C., Fault gear identification using vibration signal with discrete wavelet transform technique and fuzzy–logic inference, *Expert systems with applications*, Vol.36, pp. 3785-3794, 2009.

[24] Lei, Y. and Zuo, M., Gear crack level identification based on weighted K nearest neighbor classification algorithm, *Mechanical Systems and Signal Processing*, Vol.23, pp. 1535-1547, 2009.

[25] Lei, Y., He, Z. and Zi, Y., A new approach to intelligent fault diagnosis of rotating machinery, *Expert Systems with applications*, Vol.35, pp. 1593-1600, 2008.

[26] Yang, M. and Makis, V., ARX model-based gearbox fault detection and localization under varying load conditions, *Journal of Sound and Vibration*, Vol.329, pp. 5209-5221, 2010.

[27] Parey A., El Badaoui, M., Guillet, F. and Tandon, N., Dynamic modelling of spur gear pair and application of empirical mode decomposition-based statistical analysis for early detection of localized tooth defect, *Journal of Sound and Vibration*, Vol. 294, pp. 547-561, 2006.